Article (refereed) - postprint

Xu, Wen; Shang, Bo; Xu, Yansen; Yuan, Xiangyang; Dore, Anthony J.; Zhao, Yuanhong; Massad, Raia-Silvia; Feng, Zhaozhong. 2018. **Effects of elevated ozone concentration and nitrogen addition on ammonia stomatal compensation point in a poplar clone.** *Environmental Pollution*, 238. 760-770. https://doi.org/10.1016/j.envpol.2018.03.089

Effects of elevated ozone concentration and atmospheric nitrogen deposition on ammonia stomatal compensation point in a poplar clone

Wen Xu[1,2], Zhaozhong Feng[1,2*], Shang Bo[1,2], Yansen Xu[1,2], Xiangyang Yuan[1,2]

[1]State Key Laboratory of Urban and Regional Ecology, Research Center for Eco□Environmental Sciences, Chinese Academy of Sciences, Shuangqing Road 18, Haidian District, Beijing 100085, China.

[2]College of Resources and Environment, University of Chinese Academy of Sciences, Beijing 100049, China.

[*]Corresponding author.

E-mail address: fzz@rcees.ac.cn (Z. Feng).

Abstract: The stomatal compensation point of ammonia (χ_s) is a key factor controlling plant-atmosphere NH_3 exchange, which is dependent on the nitrogen (N) supply and varies among plant species. However, knowledge gaps remain concerning the effects of elevated atmospheric N deposition and ozone (O_3) on χ_s for forest species, resulting in large uncertainties in the parameterizations of NH_3 incorporated into atmospheric chemistry and transport models (CTMs). Here, we present a leaf-scale χ_s for hybrid poplar clone '546' (*Populusdeltoides cv. 55/56 x P. deltoides cv. Imperial*) growing in two N treatments (N0, no N added; N50, 50 kg N ha^{-1} yr^{-1} urea fertilizer added) and two O_3 treatments (CF, charcoal-filtered air; E-O_3, non-filtered air plus 40 ppb) for 126 days. Our results showed that χ_s was significantly reduced by E-O_3 (36%) but was not significantly affected by elevated N. Elevated O_3 significantly reduced the light-saturated photosynthetic rate (A_{sat}) and chlorophyll (Chl) content and significantly increased intercellular CO_2 concentrations (Ci), but had no significant effect on g_s. By contrast, elevated N significantly influenced A_{sat} but not the remaining three photosynthetic parameters. Overall, χ_s was significantly and positively corrected with A_{sat}, g_s and Chl, whereas a significant and negative relationship was observed between χ_s and Ci. Our results suggest that O_3-induced changes in A_{sat}, Ci and Chl may affect χ_s. Interactions of N and O_3 on χ_s as well as all photosynthetic parameters were not significant. Our findings provide a scientific basis for optimizing parameterizations of χ_s to respond to environmental change factors (i.e., elevated N deposition and/or O_3) in the future.

Keywords: N deposition; Ozone; Ammonia; Compensation point; Poplar

1. Introduction

Atmospheric ammonia (NH_3) is the primary alkaline trace gas in the atmosphere and plays a vital role in many biogeochemical and atmospheric processes (Behera et al., 2013). It neutralizes atmospheric acids to yield ammonium (NH_4^+) aerosols, which resulting in increased mass loadings of fine atmospheric particulate matter ($PM_{2.5}$, aerodynamic diameter ≤ 2.5) (Xu et al., 2016, 2017), thereby reducing visibility and adversely impacting ecosystem and human health (Gu et al., 2014). By contrast, atmospheric deposition of reduced N (NH_3 and NH_4^+) can cause soil acidification (Du et al., 2015), eutrophication (Pareman et al., 2016) and loss of biodiversity (Erisman et al., 2007) in sensitive ecosystems.

Plants can be either a source or a sink of atmospheric NH_3, depending on the difference between atmospheric NH_3 concentration and the so-called canopy NH_3 compensation point (Massad et al., 2010). As a major component of canopy NH_3 compensation point, Ammonia stomatal compensation point (χ_s) is defined as the atmospheric NH_3 concentration for which there is no exchange between the leaf and the atmosphere in dry conditions (Flechard et al, 2013). Theoretically, χ_s is also the air concentration in the leaf sub-stomatal cavity that is in equilibrium with ammonium concentration in the apoplast (Husted and Schjoeering, 1995). It plays a vital role in controlling the magnitude and the direction of NH_3 exchange between the canopy and the atmosphere (Sutton et al., 1995). Specifically, if atmospheric NH_3 concentrations exceed χ_s then NH_3 deposition from the atmosphere to vegetation will occur, while with atmospheric NH_3 concentrations below χ_s, there will be a net uptake of NH_3 by plants. χ_s depends directly on the plant nitrogen (N) status, developmental stage, and environmental conditions (N fertilization or atmospheric N deposition), with larger values generally observed under conditions of N supply and at senescence (Massad et al., 2009; Schjoerring et al., 1998).

χ_s can be derived from simultaneous measurement of vertical fluxes and concentrations of NH_3 by using micrometeorological flux techniques over large fields (Hansen et al., 2017; Nemitz et al., 2001; Personne et al., 2015), or in cuvettes by

finding the concentration at which the total flux is zero (Hill et al., 2001; Massad et al., 2009; Wang et al., 2011). In addition, the bioassay approach has also been developed for assessing χ_s and it is based on the determination of the leaf apoplastic NH_4^+ concentration and pH by mean of apoplast extraction (Husted and Schjørring, 1995). These two methods are complementary. Apoplast extraction is more appropriate for leaf and cell scale processes whereas chamber/micrometeorological measurements tend to be more appropriate for flux measurements at an entire plant/canopy scale (Massad et al., 2009; Sutton et al., 2009).

Forests represent a major uncertainty in quantification of regional NH_3 fluxes and parameterization of bi-directional NH_3 exchange in atmospheric chemistry and transport models (CTMs) such as AURAMS (A Unified Regional Air-quality Modelling System, Zhang et al., 2010) and CMAQ (Community Multiscale Air-Quality Modeling System, Fu et al., 2015). This is not only due to the large land area of forests but also because of the wide range of forest types and management practices. In conditions of bi-directional NH_3 exchange, forests are of particular interest. For example, temperate deciduous forests are potentially a natural source of NH_3 (Hansen et al., 2013, 2017; Neirynck and Ceulemans, 2008), leading to impact of forests on the atmospheric NH_3 level. In contrast, tropical humid forest and temperate coniferous forest can acts as net NH_3 sinks (Bertolini et al., 2016; Duyzer et al., 2005), resulting in the impact of atmospheric NH_3 on the ecological functioning of forests.

χ_s is one of the key parameters for parameterizations of NH_3 incorporated into CTMs (Massad et al., 2010). Based on published data on χ_s in relation to different plant species, growth stages, N supply etc., Massad et al. (2010) derived a new operational parameterization for integrating bi-directional NH_3 exchange into CTMs, However, uncertainties still exist for its parameterization, partially due to the following two drawbacks: 1) measurement of χ_s for different ecosystems, specific to forests, is very sparse and is only considered for a single growth stage of plants; 2) the relationships established between N fertilizer application and χ_s remain uncertain due to a lack of co-measurement of χ_s with different organic fertilizer (manure, slurry and urea) application rates. In addition, the actual parameterization of NH_3 exchange models requires large

databases accounting for the variability of χ_s. To our knowledge, there is only one process-based model developed by Riedo et al. (2002) for grasslands which accounts for the plants N nutrition and growth stage in calculating χ_s. However, as χ_s is not only driven by N input to the ecosystem and plant growth stage, it may be a strongly regulated process that depends on environmental changes such as elevated ground-level O_3.

Ground-level O_3 can be considered as the most phytotoxic air pollutant due to visible injury to a variety of plants and the rising concentrations in different regions of the world (Cooper et al., 2014; Feng et al., 2014). It affects photosynthetic parameters (e.g., stomatal conductance (g_s), light-saturated CO_2 assimilation rate (A_{sat}), intercellular CO_2 concentration (Ci) and chlorophyll (Chl) content) of forest species to a varying extent (Li et al., 2017). In contrast, atmospheric N deposition represents an important nutrient from the environment for plants (Liu et al., 2010). In N-limited ecosystems (e.g., forest) N deposition might enhance photosynthetic activity (i.e. photosynthetic enzyme activity) and net primary productivity (N fertilization effect) (Liu et al., 2011). In the context of N-saturation, However, N deposition may render plants more susceptible to pollutants and natural environmental stressors (Cardoso-Vilhena and Barnes, 2001). Such O_3 and N induced changes in the growth and metabolism of plants may affect the χ_s of plants due to a clear link between χ_s and photosynthetic parameters. For example, Mattssone and Schjoerring (1996) showed that leaf NH_3 emission from *Hordeum vulgare L. cv. Golf* plants showed a consistent diurnal pattern of photosynthesis but the opposite trend with g_s. Furthermore, Schjoerring et al. (1998) found that NH_3 emission from leaves of *Brassica napus* L plants increased with Chl degradation. Such results demonstrate that there are corresponding influences of those parameters on χ_s, which positively impacts leaf NH_3 emission (Massad et al., 2010). In this context, understanding the effects of elevated O_3 and N as well as their-driven the plant physiological controls on χ_s is important for prediction of χ_s. Unfortunately, the relevant information for different forest species is still unknown, significantly restricting the optimization of the χ_s parameter in CTM models.

Poplars are widespread deciduous plants in temperate and boreal forests. In China, poplar is a native species, with a cultivated area of more than 10 million ha (Yuan et al., 2016). We designed an experiment to investigated for the first time the individual effects of elevated N deposition (with controlled application of urea) and O_3 and their interactions on χ_s of hybrid poplar clone '546' (*Populusdeltoides cv. 55/56 x P. deltoides cv. Imperial*). In addition, we estimated the relationships between photosynthetic parameters (g_s, A_{sat}, *C*i and Chl) and χ_s, and discussed how N and O_3, as well as their-driven modifications in photosynthetic parameters (g_s, A_{sat}, *C*i and Chl), respectively affect χ_s.

2. Materials and methods

2.1. Experimental site and plant materials

The study was conducted in Yanqing Field and Experimental Basin, Tangjiapu village, Yanqing District (40°29′N, 115°59′E, 500 m.a.s.l.), about 74 km northwest of Beijing city centre. When the winds come from the north or northwest, this basin is located upwind of the Beijing urban area. The site is characterized by a continental monsoon climate, with mean annual temperature of 9 °C and mean annual precipitation of 400-500 mm.

Rooted cuttings of hybrid poplar clone '546' (*Populusdeltoides cv. 55/56 x P. deltoides cv. Imperial*) were cultivated in individual 20 L circular plastic pots on 7 May 2017. The plots were filled with local light loamy farmland soil, which was excavated at 0-10 cm depth, sieved out by a 0.3 mm pore mesh and then thoroughly mixed for homogeneity. Plants with similar height and basal stem diameter were selected and pre-adapted to open-top chambers (OTCs, octagonal base, 12.5 m^2 of growth space and 3.0 m height, covered with toughened glass) for 10 days before ozone fumigation. All seedlings were manually irrigated at 1-2 day intervals in order to keep moisture to field capacity.

2.2. O_3 and N treatments

The experiment was conducted in six OTCs with two O_3 treatments: charcoal-filtered ambient air (CF) in which ~80% of ambient O_3 was removed, and elevated O_3

(E-O_3, non-filtered air with targeted O_3 addition of 40 ppb during fumigation). Each treatment had three OTC replicates, and six potted plants were randomly distributed in each OTC. The O_3 fumigation was performed from 10 June to 22 September 2017 with day length of 10 h (from 08:00 till 18:00), except rainy days. During the fumigation period, the averaged O_3 concentrations in CF and E-O_3 were 24.0 and 80.6 ppb, respectively, and AOT40 (accumulated hourly O_3 concentration above a threshold of 40 ppb) was 2.4 and 41.6 ppm h, respectively (**Fig. 1**). Ozone was generated from pure oxygen using an electrical discharge O_3 generator (HY003, Chuangcheng Co., Jinan, China) and mixed with ambient air using a fan. Ozone concentrations inside the OTCs were continuously monitored at approximately 10 cm above the plant canopy using an ultraviolet (UV) absorption O_3 analyzer (Model 49i-Thermo, Thermo Scientific, Massachusetts, USA). The analyzers were calibrated monthly with a 49iPS calibrator (Thermo Scientific) during the experiment.

In addition to the O_3 treatments, two N treatments were applied with three replicates: control (N0, no N added), and moderate N, (N50, 50 kg N ha^{-1} yr^{-1}). For N50, N additions were applied five times (13 June, 29 June, 16 July, 1 August, 17 August) to the soil with dilute urea solutions by using a 50 mL plastic bottle and the control pots received equal amounts of pure water. In total, N50 received 0.245 g N (i.e. 0.526 g urea) throughout the experiment.

2.3. Measurements of physiological parameters

Measurements of gas exchange, leaf temperature and chlorophyll content were performed during two periods, i.e., at the end of July and August, 2017 (on 30 and 31 July, and on 29 and 31 August, respectively). For all plants, middle leaves were selected as targeted leaves, which were 11th to 13th fully expanded leaves from the apex and comprised the main part of the leaves on each plant. A portable photosynthetic system fitting with a 6400-40 leaf chamber fluorometer (LI-6400-40, LI-COR Co., USA) was used to measure gas exchange and leaf temperature from one middle leaf between 9:00 and 12:00 h. For the measurements, the photosynthetic photon flux density was set at 1200 μmol m^{-2} s^{-1}, the CO_2 concentration of air entering the leaf at 400 μmol mol^{-1} and

the relative humidity at 50-60%. The measured parameters were A_{sat}, g_s, and C_i. During the entire experimental period, a total of 72 leaf samples were measured.

Immediately after measurements of gas exchange and leaf temperature, two leaf discs were sampled from the targeted leaf and then extracted with 2 mL 95% ethanol solution in the dark for at least 72 h at 4 °C. The Chl content in the extract was determined using the specific absorption coefficients (Lichtenthaler, 1987).

2.4. Determination of apoplastic NH_4^+ and H^+ concentration

A slightly modified version of the vacuum infiltration technique developed by Husted and Schjoerring (1995) was employed to determine apoplastic NH_4^+ and H^+ concentration. Immediately after measurements of physiological parameters, the targeted leaf was cut and washed with high-purity water (18.2 Ω), in order to avoid any contamination from air pollutants (e.g., particulate NH_4^+). The leaf was then blotted dry with clean absorbent paper towel and the central petiole was removed. The leaves were separated into three replicates and then weighted, infiltrated with 280 mM sorbitol solution using a 60 mL plastic syringe with a series of vacuum/pressure for 5 min. The vacuum/pressure process was automatically applied with an intercellular fluid extractor (NS-AFE-1, Pulanta Co. Suzhou, China). The infiltrated leaves were quickly rinsed with high-purity water, blotted dry and re-weighted. The leaves were then rolled, inserted into tubes and centrifuged at 9000 r min^{-1} for 10min at 4°C to collect the apoplastic solution. Cytoplasmic contamination of the apoplast during the extraction procedure was checked by performing the extraction using a buffered solution (0.1 M Ntris[hydroxymethyl]methyl-2-aminoethanesulphonic acid, 2 mM dithiothreitol and 0.2 mM EDTA), and comparing the activity of Malate Dehydrogenase (MDH) in the apoplastic extracts to its activity in bulk tissue extracts as described by Husted and Schjørring (1995). The contamination was less than 1.2 ± 1.1% of MDH activity in apoplast extract relative to bulk tissue extract. The extracted solution was then frozen and stored at -20 °C prior to chemical analysis.

The NH_4^+ concentrations in the apoplastic extracts were measured with an AA3 continuous-flow analyzer (BranCLuebbe GmbH, Norderstedt, Germany). The

detection limit of NH_4^+ was 0.01 mg N L^{-1}. The pH of the extracted solution was measured with an InLab micro electrode (Mettler Toledo, Udorf, Switzerland). The dilution of the apoplastic solution was determined spectrophotometrically at wavelength 492 nm for the sorbitol, which allowed the calculation of a dilution factor (Hove et al., 2002). The concentration of apoplastic NH_4^+ and H^+ was corrected for dilution during the extraction procedure by multiplication with the dilution factor (F_{dil}).

The aqueous volume of the apoplast (V_{apo}, mL g^{-1} leaf fresh weight (LFW)) was estimated using the equation (Hove et al., 2002):

$$V_{apo} = \frac{V_i(F_{d,sorb}-1)}{LFW} \quad (1)$$

where V_i is the infiltration volume which was calculated by assuming a leaf density of 1 g cm^{-3} the difference in weight before and after infiltration, $F_{d,sorb}$ is the dilution factor of sorbitol.

$$F_{dil} = \frac{V_{apo}+V_{air}}{V_{apo}} \quad (2)$$

where V_{air} is the air volume inside the leaf (cm^3 g^{-1} LFW) which was measured by infiltrating leaves with low-viscosity silicone oil (10 mPa s). Based on the increase in weight and oil density (0.93 g cm^{-3}), the V_{air} was estimated to be approximately 0.16 mL g^{-1} throughout the experiment.

2.5. Determination of the leaf tissue NH_4^+ concentration

The leaf segments were cut into small pieces, frozen in a ceramic mortar with liquid N (-210 °C), and quickly ground into a homogenous powder using a ceramic pestle. The weighed samples (approximately 1.0 g per sample) were put into a 5 mL centrifuge tube with 4 mL of high-purity water, followed by centrifugation at 2000 g (4°C) for 10 min (Loubet et al., 2002). The supernatant was then decanted and filtered through a syringe filter (0.45 μm, Tengda Inc., Tianjin, China) to remove large plant tissues. The filtered solution was frozen and stored at -20 °C until analysis for NH_4^+ using an AA3 continuous-flow analyzer as mentioned before.

2.6. Calculation of NH_3 stomatal compensation point

The stomatal compensation points were derived using the apoplast pH and NH_4^+

concentrations (Loubet et al., 2002) according to the equation:

$$\chi_s = M_{NH3} \times K_H \times K_D \times \frac{[NH_4^+]}{[H^+]} \times 10^9 \qquad (3)$$

where χ_s is the stomatal compensation point in μg NH_3 m^{-3}, M_{NH3} is the molecular mass of NH_3 in g mol^{-1}, The ratio of apoplast NH_4^+ to apoplast H^+ concentration, called the emission potential (expressed as Γ_s), is temperature independent and dimensionless (Massad et al., 2010). K_H is the Henry constant and K_D is the dissociation constant. The product K_HK_D depends on temperature and was calculated following the method of (Hill et al., 2001):

$$K_HK_D = \frac{161512}{T_{leaf}} \times 10^{\frac{-4507.11}{T_{leaf}}} \qquad (4)$$

where T_{leaf} is leaf temperature in Kelvin.

2.7. Statistical analysis

Data of each investigated variable from three plants per OTC were averaged and then used as the statistical unit (N=3). Prior to analysis, all data were tested for normality using the Shapiro-Wilk's W-test and for homogeneity of variance using Levene's-test to determine whether data should be transformed to be satisfied in application. A three-way analysis of variance (ANOVA) with a mixed linear model was then conducted to examine the effects of O_3, N, measurement dates and their interactions on physiological parameters and χ_s as well as other parameters using JMP software (SAS Institute, Cary, NC, USA). Tukey's Honestly Significant Difference (HSD) test was applied to examine the significant differences. Analysis of covariance (ANCOVA) was performed to test the significance of difference in the slopes of the linear relationship between χ_s and physiological parameters using SPSS software (version 11.5; SPSS Inc., Chicago, IL, USA). Statistically significant differences were set at $P<0.05$. All the data were shown as mean ± standard deviation (SD) of three OTC replicates.

3. Results

For all investigated variables, similar and non-significant responses to E-O_3 and N50 were calculated between the two measurement dates, i.e., July and August (**Figs.**

3 and 4). Based on integrated analysis of all data from all N and O_3 treatments and the two measurement dates, the main results are presented below.

3.1. Photosynthetic parameters

The individual effects of N, O_3 and measurement date, and their interactions on A_{sat}, g_s, *C*i and Chl of the poplar clone 546 are shown in **Fig.2** and **Table 1**. For all investigated variables, the interactions of O_3 and N were not significant, but the individual effects of them were significant for most variables (**Table 1**). E-O_3 relative to CF significantly reduced A_{sat} by 55%, whereas N50 relative to N0 significantly increased A_{sat} by 6% (**Fig. 2a and Table 1**). A_{sat} significantly decreased (by 24%) in August relative to that in July, when averaged across all treatments. The effects of N and O_3 on g_s were both not significant, whereas measurement date significantly affected g_s (**Table 1, Fig. 2b**). Similar to A_{sat}, g_s significantly decreased by 30% in August compared with that in July.

Ozone significantly influenced *C*i and Chl whereas N had no significant effects on them (**Table 1, Fig. 2c, d**). *C*i was significantly increased by E-O_3 (+7%) compared with CF, and also was significantly higher (6%) in August than in July. Conversely, Chl was significantly reduced by E-O_3 (-30%), and significantly decreased (by 57%) in August.

3.2. Leaf apoplastic NH_4^+ and pH, and leaf tissue NH_4^+

Fig. 3a-c shows the responses of leaf apoplastic NH_4^+ concentration and pH, and leaf tissue NH_4^+ concentration to E-O_3 and N50. The interactions between O_3 and N and/or measurement dates were not significant for all those three variables (**Table 1**). However, individual effects of them on apoplastic NH_4^+ concentrations and pH all reached statistically significant levels. Similarly, leaf tissue NH_4^+ concentration was significantly influenced by both O_3 and measurement dates, but not by N.

Averaged apoplastic NH_4^+ concentration was significant reduced (by 15%) in E-O_3 plants compared with CF plants (**Fig. 3a, Table 1**). By contrast, the mean concentration was significantly increased (by 27%) in N50 plants compared with that

in N0 plants. A significant increase (14%) of the mean occurred in August relative to July. As for apoplastic pH, two small but significant reductions (both 4%) of the mean were found in E-O_3 and N50 plants compared with those in CF and N50 plants, respectively (**Fig. 3c, Table 1**). Also, the mean pH was significantly lower (15%) in plants grown in August than in July.

In contrast to apoplastic NH_4^+, the mean tissue NH_4^+ concentration significantly increased (by 15%) in E-O_3 plants relative to that in CF plants, whereas a small and non-significant difference in the mean was found between N0 and N50 plants (**Fig. 3b, Table 1**). The mean concentrations decreased significantly (on average by 6%) in August relative to July.

3.3. Emission potential (Γ_s) and stomatal compensation point (χ_s)

As presented in Table 1, both O_3 and measurement dates significantly affected Γ_s, whereas N had no significant effect on it. Also, no significant interactions between O_3, N and/or measurement dates were observed. E-O_3 treatment relative to CF significantly reduced Γ_s by 39% (**Fig. 3d**). Γ_s was significantly reduced (by 85%) in August compared with that in July.

Similar to Γ_s, χ_s was significantly lower in E-O_3 than in CF (0.29 ± 0.29 and 0.48 ± 0.45 μg NH_3 m^{-3}), and also in August than in July (0.07 ± 0.05 and 0.70 ± 0.29 μg NH_3 m^{-3}) (**Fig. 4**). However, it is noteworthy that the effect of N and its interaction with O_3 on χ_s were marginally significant (both P=0.059) (**Table 1**).

3.4. Correlations between stomatal compensation point (χ_s) and photosynthetic parameters

χ_s was positively and significantly correlated with A_{sat}, g_s and Chl (**Fig. 5a, b,d**), whereas a negative and significant correlation between χ_s and Ci was observed (**Fig. 5c**). ANCOVA results did not show significant differences in the slope of the regression lines for the individual O_3 or N treatments.

4. Discussion

4.1. Effect of N application

The application rate of urea fertilizer in the present experiment (50 kg N ha^{-1} yr^{-1}) is approximately 2.3 and 3 times higher than the averages of N deposition over China (16 kg N ha^{-1} yr^{-1} in 2008-2012 period, Zhao et al., 2017) and in China's forests (22 kg N ha^{-1} yr^{-1} in 1995-2010 period, Du et al., 2014), respectively. It is also approximately 1.7-5.0 times greater than reported values during recent years in the N deposition hotspots of western Europe (20.0 to 28.1 kg N ha^{-1} yr^{-1}, Vet et al., 2014), and North America (10.0 to 20.0 kg N ha^{-1} yr^{-1}, Li et al., 2016). According to Liu et al. (2013), N deposition increased by approximately 8 kg N ha^{-1} yr^{-1} between the 1980s and the 2000s in China. Also, total N deposition is expected to have a 5%-10% increase in the year 2050 relative to 2005 (Kanakidou et al., 2016). In view of the above, the level of N addition in this study is sufficient to assess the ecological effects of enhanced N deposition expected in the future.

Apoplastic NH_4^+ concentration is one of the key factors in controlling χ_s, which is associated with the status of leaf N and external N supply (e.g., N fertilization and atmospheric deposition) (Herrmann et al., 2009; Massad et al., 2008). The apoplastic NH_4^+ concentrations measured for the N0 and N50 treatments (but without E-O_3) were 0.10 ± 0.01 and 0.13 ± 0.01 mM, respectively (**Fig. 3a**). To our knowledge published data on apoplastic NH_4^+ concentrations in leaves of poplar 546 is unavailable, making a direct comparison with other studies impossible. However, our measured value for N0 treatments were close to that reported for *Fagus sylvatica* growing in July and August (0.11 mM, Wang et al., 2011). Compared with agricultural crops, our measured value for N0 treatments was higher than that reported for barley (0.04 mM, Mattsson et al., 1998), and was close to the value of 0.10 measured for oilseed rape (Massad et al., 2009) both growing on N0. The value for plants grown on N50 was similar to that measured for oilseed rape (0.18 mM with 6 mM NO_3^-, Schjoerring et al., 2002), and was lower than the value of 1.9 mM observed for barley grown on 5 mM NH_4^+ (Mattsson et al., 1998). As expected, enhanced N input (N50) significantly increased the apoplastic NH_4^+ concentration (**Fig. 2, Table 1**), probably due to increased soil N

availability. This result is similar to the findings of Massad et al. (2009) that the NH_4^+ concentrations in leaf apoplast of oilseed rape increased significantly with rising N treatments (aside from NO_3^- supply).

Besides apoplastic NH_4^+ concentration, the pH of the apoplast may be the most important factor determining χ_s. There is evidence that NH_4^+-fed plants have reduced apoplastic pH compared to NO_3^--fed plants, e.g., sunflower (Hoffmann et al., 1992), soybean (Kosegarten and Englisch, 1994) and barley (Mattsson et al., 1998), probably due to a root rather than shoot assimilation of N (Pearson et al., 1998). Application of urea fertilizer in the present experiment probably enhanced soil NH_4^+ level via urea hydrolysis, which further significantly increased apoplastic NH_4^+ concentrations (**Fig. 3a**) via root assimilation and the subsequent transport of NH_4^+ to the foliar apoplast in the xylem (Mattson et al., 1998). This behaviour, along with NH_4^+ uptake-induced acidification may offer an explanation for lower apoplastic pH (ranging from 4.6 to 6.0, **Fig. 3c**) of poplar 546 compared with those reported for most plant species (between 5.0 and 6.5, Grignon and Sentenac, 1991).

Enhanced N input significantly increased both apoplastic NH_4^+ and H^+ concentration with a similar significant level (**Figs. 3a,c and Table 1**) This may partly explain why N has no significant effect on χ_s. This, together with the relatively low calculated χ_s throughout, especially in August (**Fig. 4**), suggest that χ_s appears to be pH-driven in this study. The apoplastic pH of *Phaseolus vulgaris* has been found to become alkalinized during photosynthesis (Raven and Farquhar, 1989). Similarly, we found that the N load significantly increased A_{sat} of poplar 546 (**Fig. 2a, Table 1**), which significantly positively correlated with apoplastic pH (**Fig. 6a**) but had no significant relationship with apoplastic NH_4^+ concentration (R^2=0.09, P=0.141). These results provide an explanation for a significant and positive relationship observed between A_{sat} and χ_s (**Fig. 5a**). Although such an increase in apoplastic pH occurred due to increased A_{sat} by N load, it is insufficient to offset NH_4^+ uptake-induced apoplast acidification, leading to relatively low χ_s.

4.2. Effect of O_3 application

According to monitoring results for the 2014-2016 period in 187 Chinese cities, the mean daily 8-h O_3 concentrations peak in summer reached up to 114.30 ± 23.78 ppb (Li et al., 2017). Obviously, the O_3 level in E-O_3 was within the range of current O_3 levels in China and was also in the range of future expected concentrations in warm and sunny areas of the world at the end of this century (The Royal Society 2008; IPCC 2013). The dose of O_3 (41.6 ppm h in AOT40, **Fig. 1**) in E-O_3 by far exceeded the O_3 exposure limit of 5 ppm h for forest protection (CLRTAP, 2015) and 12 ppm h for poplar protection (Hu et al., 2015). As anticipated, O_3-induced injuries to poplar 546 were detected in E-O_3 despite N fertilization (e.g., reduction of A_{sat} and Chl, **Fig. 2a, d**), thus confirming that poplar 546 is a very sensitive species to O_3 (Shang et al., 2017).

E-O_3 significantly increased *C*i and decreased A_{sat} and Chl, respectively, but did not significantly affect g_s (**Figs. 2 and Table 1**). These results are consistent with the findings of Shang et al. (2017) for polar 546. Similarly, a previous study showed that O_3 can substantially reduce A_{sat} in most plants, and also detected an uncoupled relationships between A_{sat} and g_s (Zhang et al., 2012). This can be explained by the fact that the O_3-induced reduction in A_{sat} is largely ascribed to non-stomatal factors, i.e. impaired physiological activity of mesophyll cells (Akhtar et al., 2010; Feng et al., 2016).

We found that E-O_3 significantly reduced the calculated χ_s (**Fig. 4**). This is most likely related to a decline in apoplastic pH resulting from O_3-induced changes in photosynthetic parameters, i.e., decreased A_{sat} and Chl, and increased *C*i (**Fig. 2a,c,d, Table 1**). This is because in addition to A_{sat}, both Chl and *C*i correlated significantly with χ_s and apoplastic pH (Figs. **5c,d** and **6c,d**). In addition, there was a large response of apoplastic NH_4^+ to photosynthesis (Mattsson and Schjoerring, 1996), mainly due to the fact that NH_3 assimilation by plants requires carbon skeletons generated from photosynthesized carbohydrates for the synthesis of amino acids (Huppe and Turpin, 1994). In this regard, a significant reduction in A_{sat} can also give rise to declines in apoplastic NH_4^+ concentration. Similar to N, ozone has a greater impact on apoplastic pH than on apoplastic NH_4^+ concentration, as demonstrated by the significant reduction of Γ_s by O_3 (**Fig. 3d, Table 1**); this therefore led to a significant reduction in χ_s (**Fig. 4,**

Table 1).

4.3. Dependence on measurement date

χ_s can be influenced by plant developmental stage since leaf apoplastic NH_4^+ concentration and pH varies among leaves of different ages (Hill et al., 2002). Mattsson and Schjoerring (2003) reported that, for ryegrass (*Lolium perenne*), both apoplastic and tissue NH_4^+ concentrations were 2-3 times higher in intact leaves (with visual symptoms of senescence) compared with green leaves. The present study shows that leaf apoplastic NH_4^+ concentrations significantly increased in August compared with those in July, whereas a significant reduction was found for leaf tissue NH_4^+ concentration (**Fig. 3a, b**). In addition, a negative and marginally significant (P=0.053) relationship was observed between NH_4^+ concentrations in apoplast and in tissue (**Fig. 6d**). These results together indicated that NH_4^+ is actively transported from the leaf tissue to the apoplast. This explanation is supported by evidences from earlier studies showing that apoplastic fluid in leaves constitutes a highly dynamic NH_4^+ pool, to which NH_4^+ is constantly supplied via NH_3 efflux from the mesophyll cells (Nielsen and Schjoerring, 1998; Schjoerring et al. 2000).

Regarding apoplastic pH, the values measured in August were significantly reduced compared to July, and almost all were <5 (**Fig. 3c, Table 1**), for which an explanation is the combined effect of NH_4^+ uptake-induced acidification (see Sect. 4.1) and O_3-accelerated leaf senescence (Gao et al., 2017). As reported by Mattsson and Schjoerring (2003), leaf aging from green leaves to yellow tips resulted in a pronounced decrease of pH by more than 1 unit. Thus, a significantly lower A_{sat} in August resulting from accelerated leaf senescence (**Fig. 2a, Table 1**) also contributed to lower apoplastic pH due to the existence of apoplast alkalinizion during photosynthesis as mentioned earlier.

χ_s was significantly reduced in August compared with July (**Fig. 4**). This is likely due to the greater impact of measurement date on apoplastic pH than on apoplastic NH_4^+ concentration as indicated by their respective significant level (**Table 1**). The change in stomatal opening is an important control mechanism for the regulation of

influxes and outfluxes of NH_3 into or out of the leaves because the conductance for diffusion of NH_3 is affected (Schjoerrin et al., 1998). We found that g_s significantly decreased in August (**Fig. 2b, Table 1**). Also, a positive and significant relationship was observed between g_s and χ_s (**Fig. 5b**); this is mainly caused by measurement date as both E-O_3 and N did not significantly affect g_s. These results together suggested that a significant reduction of g_s also contributed to a reduction in χ_s.

4.4. Uncertainty and recommendations

In the present study, χ_s is calculated based on direct measurements of leaf apoplastic NH_4^+ concentration and pH by means of extraction of the apoplastic fluid with successive vacuum infiltration/centrifugation technique (Husted and Schjørring., 1995). Although this technique has been successfully applied to several plant species in the field (Herrmann et al., 2009; Mattsson et al., 2009), it is subject to uncertainties regarding potential regulation of apoplastic NH_4^+ concentration and pH by the plant during the infiltration and buffering effects (Massad et al., 2009). For example, Nielsen and Schjørring (1998) showed that apoplastic NH_4^+ concentration in *Brassica napus* L. appeared to be regulated during infiltration. However, Hill et al. (2001) did not detect such a homeostasis for apoplastic NH_4^+ concentration in *Luzula sylvatica* (Huds.) Gaud. Following the method of van Hove et al. (2002), F_{dil}, calculated based on determination of V_{air} and V_{apo} (**Equ. 2**), was applied to correct apoplastic concentrations. V_{apo} values obtained in the present work varied from 0.06 to 0.23. These values fit well into the range found by other researcers for different plant species (Van Han et al., 2001, 2002). The measured V_{air} (0.16 ml g^{-1} LFW) was also comparable to values (0.21 mL g^{-1} LFW) reported for *Lolium perenne L.* (Van Han et al., 2002). These results indicate that the value for F_{dil} determined in the present study was acceptable. However, due to a lack of information regarding infiltration of poplar 546, use of F_{dil} might also result in some uncertainties in apoplastic NH_4^+ concentrations and pH, and probably in χ_s if there is a potential difference in the buffering capacity between them.

The vacuum infiltration/centrifugation method is also subject to some uncertainty due to the strong possibility of cytoplasmic contamination of the apoplast during the

extraction procedure (Lohaus et al., 2001). We estimated the error in this method by assaying the contamination of the apoplast by MDH activity. The cytoplasmic contamination in the present work was about 1.2%.

χ_s obtained in the current study was calculated at the leaf scale and only for the middle leaf position. However, χ_s may differ significantly depending on leaf position (e.g., upper, middle and lower) due to difference in the N status of the leaves. Thus, the resulting effects of enhanced N and O_3 on χ_s are not enough to represent the characteristics of the entire-plant. Furthermore, the present experiment was designed based on OTC chambers. However, OTCs have effects of their own, such as differences in microclimate (e.g., air temperature andhumidity), fixed gas flow and limited space, which could over-estimatedor under-estimate the effects of O_3 on plants (Feng et al., 2010). Note that χ_s is shown to be influenced by air temperature, partly by affecting the amount of NH_3 dissolved in the apoplast, and partly by affecting the leaf tissue NH_4^+ generation (or assimilation)-associated physiological processes (Schjoerring et al. 1998). To more accurately assess the effects of N, O_3 and/or plant growth stage on χ_s, at least the two following developments are recommended in future work: 1) to employ open-air fumigations (O_3-FACE systems, Paoletti et al., 2016), and 2) to investigate vertical profile of χ_s at plant scale

.

4.5. Implications

For forest ecosystems, χ_s is commonly expected to increase considerably with input of the different types of N fertilizer applied (nitrate, ammonium or ammonium nitrate) (Massad et al., 2010). We demonstrate that urea addition did not significantly affect χ_s of forest species (i.e., poplar 546) (note however that the resulting reduction reached marginal significant level, P=0.059) (**Fig. 4, Table 1**). χ_s is affected by the plant's development stage and may peak at senescence, which is especially true for agricultural crops (Hill et al., 2002; Mattsson and Schjoerring, 2003). We find that there is a significant reduction of χ_s for forest species (i.e., poplar 546) in the context of O_3-accelerated senescence. Based on these findings, we propose that current parameterizations of χ_s in chemical transport models should be inoptimized to partially

respond to changes in environmental conditions (e.g., elevated N and/or O_3). In addition, χ_s is a highly variable parameter, influenced by a range of physiological conditions (Schjoerrin et al., 1998). We found that A_{sat}, g_s and Chl significantly and positively corrected with χ_s, whereas a significant and negative relationship was observed between *C*i and χ_s (**Fig. 5**). Understanding these physiological controls of χ_s is essential for modeling its dynamic behaviour.

Our selected poplar 546 belongs to deciduous broadleaf species. To preliminarily assess whether Chinese deciduous broadleaf forests (**Fig. 7a**) act as a source or a sink for atmospheric NH_3, we compared the calculated χ_s for elevated N and O_3 treatment (N50*E-O_3) in July (average 0.54 μg NH_3 m^{-3}) and August (average 0.03 μg NH_3 m^{-3}) with modeled atmospheric NH_3 concentration in July (**Fig. 7b**) and August (**Fig. 7c**) during 2008-2012 period (which was modeled using the GEOS-Chem model and fitted well with the surface NH_3 measurements, see details in Zhao et al. (2017)). The results of the comparison show that the modeled NH_3 concentrations over approximately 91% and 100% of total land area exceeded the corresponding χ_s in July and August, respectively. It should be noted that such percentages are considered to be approximate estimates, as χ_s may vary among different forest species, and the current atmospheric NH_3 concentration cannot represent future NH_3 levels. Nevertheless, we may conclude that under the current ambient NH_3 concentrations in China the canopy of deciduous broadleaf forests is unlikely to be a major source of NH_3 emission during summertime.

5. Conclusions

This study is the first time to investigate the combined effects of O_3 exposure and N load on χ_s of forest species. Our results demonstrated that elevated O_3 significant reduced χ_s, in tandem with A_{sat}, *C*i and Chl, while use of urea as N load had no significant effect on χ_s. The interaction of O_3 exposure and N load on χ_s were not significant. These results provide underpinning data for optimizing the parameterizations of χ_s in the CTMs, allowing response to global change variables (i.e., atmospheric N deposition and O_3).

Acknowledgments

This study was supported by the National Key R&D Program of China (2017YFC0210106), the National Natural Science Foundation of China (41705130)

References

Akhtar, N., Yamaguchi, M., Inada, H., Hoshino, D., Kondo, T., Izuta, T., 2010. Effects of ozone on growth, yield and leaf gas exchange rates of two Bangladeshi cultivars of wheat (*Triticum aestivum L.*). Environ. Pollut. 158, 1763–1767.

Behera, S.N., Sharma, M., Aneja, V.P., Balasubramanian, R., 2013. Ammonia in the atmosphere: a review on emission sources, atmospheric chemistry and deposition on terrestrial bodies. Environ. Sci. Pollut. R. 20(11), 8092–8131.

Bertolini, T., Flechard, C.R., Fattore, F., Nicolini, G., Stefani, P., Materia, S., Valentini, R., Vaglio L.G., Castaldi, S., 2016. DRY and BULK atmospheric nitrogen deposition to a West-African humid forest exposed to terrestrial and oceanic sources. Agr. Forest Meteor. 218–219, 184–195.

Cardoso-Vilhena, J., Barnes, J., 2001. Does nitrogen supply affect the response of wheat (Triticum aestivum cv. Hanno) to the combination of elevated CO_2 and O_3? J. Exp. Bot. 52, 1901–1911.

CLRTAR, 2015. Chapter 3: Mapping critical levels for vegetation. Manual on methodologies and criteria for modelling and mapping critical loads & levels and air pollution effects, risks and trends. Manual on Methodologies and Criteria for Modelling and Mapping Critical Loads and Levels and Air Pollution Effects, Risks and Trends. United Nations Economic Commission for Europe (UNECE)

Convention on Long-range Transboundary Air Pollution, Geneva (URL:http://www.icpmapping.org).

Cooper, O.R., Parrish, D.D., Ziemke, J., Balashov, N.V., Cupeiro, M., Galbally, I.E., Gilge, S., Horowitz, L., Jensen, N.R., Lamarque, J.F., Naik, V., Oltmans, S.J., Schwab, J., Shindell, D.T., Thouret, V., Wang, Y., Zbinden, R.M., 2014. Global distribution and trends of tropospheric ozone: An observation-based review. Elementa Science of the Anthropocene 2, 000029, dio: : 10.12952/journal.elementa.000029.

Du, E., Jiang, Y., Fang, J.Y., de Vries, W., 2014. Inorganic nitrogen deposition in China's forests: Status and characteristics. Atmos. Environ. 98(98), 474–482.

Du, E., de Vries, W., Liu, X., Fang, J., Galloway, J. N., Jiang, Y., 2015. Spatial boundary of urban 'acid islands' in southern China. Sci. Rep. 5, 12635.

Duyzer, J., Pilegaard, K., Simpson, D., Weststrate, H., Walton, S., 2005. A simple model to estimate exchange rates of nitrogen dioxide between the atmosphere and forests. Biogeosciences Discuss. 2, 1033–1065.

Erisman, J.W., Bleeker, A., Galloway, J., Sutton, M.S., 2007. Reduced nitrogen in ecology and the environment. Environ. Pollut. 150(1), 140–149.

Flechard, C. R., Massad, R. S., Loubet, B., Personne, E., Simpson, D., Bash, J. O., Cooter, E. J., Nemitz, E., Sutton, M. A., 2013. Advances in understanding, models and parameterizations of biosphere-atmosphere ammonia exchange. Biogeosciences 10(7), 5183–5225.

Feng, Z.Z., Wang, S.G., Szantoic, Z., Chen, S.A., Wang, X.K., 2010. Protection of plants from ambient ozone by applications of ethylenediurea (EDU): A meta-analytic review. Environ. Pollut. 158(10), 3236–3242.

Feng, Z.Z., Sun, J.S., Wan, W.X., Hu, E.Z., Calatayud, V., 2014. Evidence of widespread ozone-induced visible injury on plants in Beijing, China. Environ. Pollut. 193(1), 296–301.

Feng, Z.Z., Wang, L., Pleijel, H., Zhu, J.G., Kobayashi, K., 2016. Differential effects of ozone on photosynthesis of winter wheat among cultivars depend on antioxidative enzymes rather than stomatal conductance. Sci. Total Environ. 572, 404–411.

Flechard, C.R., Massad, R.S., Loubet, B., Personne, E., Simpson, D., Bash, J.O., Cooter, E.J., Nemitz, E., Sutton, M.A., 2011. Advances in understanding, models and parameterizations of biosphere-atmosphere ammonia exchange. Biogeosciences 10(7), 5183–5225.

Gao, F., Catalayud, V., Paoletti, E., Hoshika, Y., Feng, Z.Z., 2017. Water stress mitigates the negative effects of ozone on photosynthesis and biomass in poplar plants. Environ. Pollut. 230, 268–279.

Grignon, C., Sentenac, H., 1991. pH and ionic conditions in the apoplast. Annu. Rev. Plant Biol. 42, 103–128.

Gu, B.J., Sutton, M.A., Chang, S.X., Ge, Y., Jie, C., 2014. Agricultural ammonia emissions contribute to China's urban air pollution. Front. Ecol. Environ. 12(5), 265–266.

Hansen, K., Sørensen, L.L., Hertel, O., Geels, C., Skjøth, C.A., Jensen, B., Boegh, E., 2013. Ammonia emissions from deciduous forest after leaf fall. Biogeosciences 10, 4577–4589.

Hansen, K., Personne, E., Skjøth, C.A., Loubet, B., Ibrom, A., Jensen, R., Sørensen, L.L., Boegh, E., 2017. Investigating sources of measured forest-atmosphere ammonia fluxes using two-layer bi-directional modeling. Agr. Forest Meteor. 237–238, 80–94.

Herrmann, B., Mattsson, M., Jones, S. K., Cellier, P., Milford, C., Sutton, M. A., Schjoerring, J. K., Neftel, A., 2009. Vertical structure and diurnal variability of ammonia exchange potential within an intensively managed grass canopy. Biogeosciences 6(1), 15–23.

Hill, P.W., Raven, J.A., Loubet, B., Fowler, D., Sutton, M.A., 2001. Comparison of gas exchange and bioassay determinations of the ammonia compensation point in *Luzula sylvatica*, (Huds.) Gaud. Plant Phys. 125, 476–487.

Hill, P.W., Raven, J.A., Sutton, M.A., 2002. Leaf age-related differences in apoplastic NH_4^+ concentration, pH and the NH_3 compensation point for a wild perennial. J. Exp. Bot. 53(367), 277–286.

Hoffmann, B., Planker, R., Mengel, K., 1992. Measurements of pH in the apoplast of

sunflower leaves by means of fluorescence. Physiol. Plantarum 84, 146–153.

Hu, E.Z., Gao, F., Xin, Y., Jia, H.X., Li, K.H., Hu, J.J., Feng, Z.Z., 2015. Concentration- and fluxbased ozone dose-response relationships for five poplar clones grown in North China. Environ. Pollut. 207, 21–30.

Huppe, H.C., Turpin, D.H., 1994. Integration of carbon and nitrogen metabolism in plant and algal cells. Annu. Rev. Plant Biol. 45(1), 577–607

Husted, S., Schjoerring, J. K., 1995. Apoplastic pH and Ammonium Concentration in Leaves of Brassica napus L. Plant Physiol. 109(4), 1453–1460.

IPCC, 2013. Climate Change 2007: The Physical Science Basis. In Contribution of Working Group I to the Fifth Assessment Report of the Intergovernmental Panel on Climate Change. Intergovernmental Panel on Climate Change (eds Stocker T.F., Qin D., Plattner G.K., Tignor M.M.B., Allen S.K., Boschung J., et al.), pp. 1552, Cambridge University Press, Cambridge, United Kingdom and New York, NY, USA.

Kanakidou, M., Myriokefalitakis, S., Daskalakis, N., Fanourgakis, G., 2016. Past, present, and future atmospheric nitrogen deposition. J. Atmos. Sci. 73 (5), 160303130433005.

Kosegarten, H., Englisch, G., 1994. Effect of various nitrogen forms on the pH in leaf apoplast and on iron chlorosis of Glycine max L. J. Plant Nutr. Soil Sc. 157(6), 401–405.

Li, P., Feng, Z.Z., Catalayud, V., Yuan, X.Y., Xu, Y.S., Paoletti, E., 2017. A meta-analysis on growth, physiological, and biochemical responses of woody species to ground-level ozone highlights the role of plant functional types. Plant Cell Environ. 40(10), 2369–2380.

Li, Y., Schichtel, B.A., Walker, J.T., Schwede, D.B., Chen, X., Lehmann, C.M., Puchalski, M.A., Gay, D.A., Collett, J.L., 2016. Increasing importance of deposition of reduced nitrogen in the United States. Proc. Natl. Acad. Sci. U.S.A. 113 (21), 5874.

Lichtenthaler, H.K., 1987. [34] Chlorophylls and carotenoids: pigments of photosynthetic biomembranes. Methods Enzym. 148, 350–382.

Liu, X.J., Song, L., He, C.E., Zhang, F.S., 2010. Nitrogen deposition as an important nutrient from the environment and its impact on ecosystems in China. J Arid Land

2(2), 137–143.

Liu, X.J., Duan, L., Mo, J.M., Du, E.Z., Shen, J.L., Lu, X.K., Zhang, Y., Zhou, X.B., He, C.E., Zhang, F.S., 2011. Nitrogen deposition and its ecological impact in China: an overview. Environ. Pollut. 159(10), 2251–2264.

Lohaus, G., Pennewiss, K., Sattelmacher, B., Hussmann, M., Muehling, K.H., 2001. Is the infiltration–centrifugation technique appropriate for the isolation of apoplastic fluid? A critical evaluation with different plant species. Physiol. Plantarum 111(4), 457–465.

Loubet, B., Milford, C., Hill, P.W., Tang, Y. S., Cellier, P., Sutton, M.A., 2002. Seasonal variability of apoplastic NH_4^+ and pH in an intensively managed grassland. Plant Soil 238(1), 97–110.

Massad, R.S., Loubet, B., Tuzet, A., Cellier, P., 2008. Relationship between ammonia stomatal compensation point and nitrogen metabolism in arable crops: Current status of knowledge and potential modelling approaches. Environ. Pollut. 154(3), 390–403.

Massad, R.S., Loubet, B., Tuzet, A., Autret, H., Cellier, P., 2009. Ammonia stomatal compensation point of young oilseed rape leaves during dark/light cycles under various nitrogen nutritions. Agr. Ecosyst. Enviro. 133(3), 170–182.

Massad, R.S., Nemitz, E., Sutton, M.A., 2010. Review and parameterisation of bi-directional ammonia exchange between vegetation and the atmosphere. Atmos. Chem. Phys. 10(21), 10359–10386.

Mattsson, M., Schjoerring, J., 1996. Ammonia emission from young barley plants: influence of N source, light/dark cycles and inhibition of glutamine synthetase. J. Exp. Bot. 47(4), 477–484.

Mattsson, M., Husted, S., Schjoerring, J.K., 1998. Influence of nitrogen nutrition and metabolism on ammonia volatilization in plants. Nutr. Cycl. Agroecosys. 51(1), 35–40.

Mattsson, M., Schjoerring, J. K., 2003. Senescence-induced changes in apoplastic and bulk tissue ammonia concentrations of ryegrass leaves. New Phytol. 160(3), 489–499.

Mattsson, M., Herrmann, B., David, M., Loubet, B., Riedo, M., Theobald, M.R., Sutton,

M.A., Bruhn, D., Neftel, A., Schjoerring, J.K., 2009. Temporal variability in bioassays of the stomatal ammonia compensation point in relation to plant and soil nitrogen parameters in intensively managed grassland. Biogeosciences 6(2), 171–179.

Neirynck, J. and Ceulemans, R., 2008. Bidirectional ammonia exchange above a mixed coniferous forest. Environ. Pollut. 154, 424–438.

Nemitz, E., Flynn, M., Williams, P.I., Milford, C., Theobald, M.R., Blatter, A., Gallagher, M.W., Sutton, M.A., 2001. A relaxed eddy accumulation system for the automated measurement of atmospheric ammonia fluxes. Water Air Soil Pollut. Focus 1(5–6), 189–202.

Nielsen, K.H., Schjoerring, J.K., 1998. Regulation of apoplastic NH_4^+ concentration in leaves of oilseed rape. Plant Physiol. 118(4), 1361–1368.

Pakeman, R.J., Alexander, J., Brooker, R., Cummins, R., Fielding, D., Gore, S., Hewison, R., Mitchell, R., Moore, E., Orford, K., 2016. Long-term impacts of nitrogen deposition on coastal plant communities. Environ. Pollut. 212, 337–347.

Paoletti, E., Materassi, A., Fasano, G., Hoshika, Y., Carriero, G., Silaghi, D., Badea, O., 2016. A new-generation 3D ozone FACE (Free Air Controlled Exposure). Sci. Total Environ. 575, 1407–1414.

Pearson, J., Clough, E.C.M., Woodall, L.J., Havill, D.C., Zhang, X.-H., 1998. Ammonia emissions to the atmosphere from leaves of wild plants and Hordeum vulgare treated with methionine sulphoximine. New Phytol. 138, 37–48.

Personne, E., Tardy, F., Génermont, S., Decuq, C., Gueudet, J.C., Mascher, N., Durand, B., Masson, S., Lauransot, M., Fléchard, C., Burkhardt J., Loubet B., 2015. Investigating sources and sinks for ammonia exchanges between the atmosphere and a wheat canopy following slurry application with trailing hose. Agr. Forest Meteor. 207, 11–23.

Raven J.A., Farquhar G.D., 1989. Leaf apoplast pH estimation in Phaseolus vulgaris. In: Dainty J, Michelis MI, MarrèE, Rasi-Caldogno F, eds. Plant membrane transport: the current position. Amsterdam: Elsevier, 607–610.

Riedo, M., Milford, C., Schmid, M., Sutton, M.A., 2002. Coupling soil-plant -

atmosphere exchange of ammonia with ecosystem functioning in grasslands. Ecol. Model. 158(1-2), 83–110.

Schjoerring, J.K., Mattsson, M., Husted, S., 1998. Physiological parameters controlling plant-atmosphere ammonia exchange. Atmos. Environ. 32(3): 491-498.

Schjoerring, J.K., Husted, S.M.G., Nielsen, K., Finnemann, J. Matt, M., 2000. Physiological regulation of plant-atmosphere ammonia exchange. Plant Soil 221(1), 95-102.

Schjoerring, J.K., Husted, S., Mack, G., Mattsson, M., 2002. The regulation of ammonium translocation in plants. J. Exp. Bot. 53(370), 883–890.

Shang, B., Feng, Z.Z., Li, P., Yuan, X.Y., Xu, Y.S., Calatayud, V., 2017. Ozone exposureand flux-based response relationships with photosynthesis, leaf morphology and biomass in two poplar clones. Sci. Total Enviro 603–604, 185–195.

Sutton, M.A., Schjoerring, J.K., Wyers, G.P., 1995. Plant atmosphere exchange of ammonia. Philos. T. Roy. Soc. S-A. 351, 261–278.

Sutton, M.A., Nemitz, E., Milford, C., Campbell, C., Erisman, J.W., Hensen, A., Cellier, P., David, M., Loubet, B., Personne, E., Schjoerring, J.K., Mattsson, M., Dorsey, J.R., Gallagher, M.W., Horvath, L., Weidinger, T., Meszaros, R., Dämmgen, U., Neftel, A., Herrmann, B., Lehman, B.E., Flechard, C., Burkhardt, J., 2009. Dynamics of ammonia exchange with cut grassland: synthesis of results and conclusions of the GRAMINAE Integrated Experiment. Biogeosciences 6(12), 2907–2934.

The Royal Society, 2008. Ground-level ozone in the 21st century: future trends, impacts and policy implications. Science Policy Report 15/08. The Royal Society, London.

Van Hove, L. W. A., Heeres, P., Bossen, M. E., 2002. The annual variation in stomatal ammonia compensation point of rye grass (*Lolium perenne L.*) leaves in an intensively managed grassland. Atmos. Environ. 36(18), 2965-2977.

Vet, R., Artz, R.S., Carou, S., Shaw, M., Ro, C.-U., Aas, W., Baker, A., Bowersox, V.C., Dentener, F., Galy-Lacaux, C., Hou, A., Pienaar, J.J., Gillett, R., Cristina Forti, M., Gromov, S., Hara, H., Khodzher, T., Mahowald, N.M., Nickovic, S., Rao, P.S.P., Reid, N.W., 2014. A globle assessment of precipitation, chemistry and deposition of sulfur, nitrogen, sea salt, base cations, organic acids, acidity and pH, and phosphorus.

Atmos. Environ. 93 (3–4), 3–100.

Wang, L., Xu, Y.C., Schjoerring, J.K., 2011. Seasonal variation in ammonia compensation point and nitrogen pools in beech leaves (*Fagus sylvatica*). Plant Soil 343 (1-2), 51–66.

Xu, W., Luo, X.S., Pan, Y.P., Zhang, L., Tang, A.H., Shen, J.L., Zhang, Y., Li, K.H., Wu, Q.H., Yang, D.W., Zhang, Y.Y., Xue, J., Li, W.Q., Li, Q.Q., Tang, L., Lu, S.H., Liang, T., Tong, Y.A., Liu, P., Zhang, Q., Xiong, Z.Q., Shi, X.J., Wu, L.H., Shi, W.Q., Tian, K., Zhong, X.H., Shi, K., Tang, Q.Y., Zhang, L.J., Huang, J.L., He, C.E., Kuang, F.H., Zhu, B., Liu, H., Jin, X., Xin, Y.J., Shi, X.K., Du, E.Z., Dore, A.J., Tang, S., Collett, J.L., Goulding, K., Sun, Y.X., Ren, J., Zhang, F.S., Liu, X.J., 2015. Quantifying atmospheric nitrogen deposition through a nationwide monitoring network across China. Atmos. Chem. Phys. 15, 12345–12360.

Xu, W., Wu, Q.H., Liu, X.J., Tang, A.H., Dore, A., Heal, M., 2016. Characteristics of ammonia, acid gases, and $PM_{2.5}$ for three typical land-use types in the North China Plain. Environ. Sci. Pollut. R. 23(2), 1158–1172.

Xu, W., Song, W., Zhang, Y., Liu, X., Zhang, L., Zhao, Y., Liu, D., Tang, A., Yang, D., Wang, D., 2017. Air quality improvement in a megacity: implications from 2015 Beijing Parade Blue pollution control actions. Atmos. Chem. Phys. 17, 31–46.

Yuan, X.Y., Calatayud, V., Gao, F., Fares, S., Paoletti, E., Tian, Y., Feng, Z.Z., 2016. Interaction of drought and ozone exposure on isoprene emission from extensively cultivated poplar. Plant Cell Environ. 39(10):2276.

Zhang, L., Wright, P. L., Asman, W. A. H., 2010. Bi-directional air-surface exchange of atmospheric ammonia – A review of measurements and a development of a big-leaf model for applications in regional-scale air-quality models. J. Geophys. Res., 115, D20310, doi:10.1029/2009JD013589.

Zhang, W.W., Feng, Z.Z., Wang, X.K., Niu, J.F., 2012. Responses of native broadleaved woody species to elevated ozone in subtropical China. Environ. Pollut. 163(4), 149–157.

Zhao, Y., Zhang, L., Chen, Y.F., Liu, X.J., Xu, W., Pan, Y.P., Duan, L., 2017. Atmospheric nitrogen deposition to China: a model analysis on nitrogen budget and

critical load exceedance. Atmos. Environ. 153, 32–40.

Figure captions

Figure 1. The 10 h (8:00-18:00) mean O_3 concentrations (ppb) and AOT40 (ppm h) from 10 June to 22 September 2017 in charcoal-filtered air (CF) and elevated O_3 (E-O_3) treatments.

Figure 2. Effects of ozone (CF, charcoal-filtered ambient air, and E-O_3, elevated O_3) and Nitrogen (N0, no N added, and N50, 50 kg N ha^{-1} yr^{-1}) on light-saturated photosynthesis (A_{sat}), stomatal conductance (g_s), intercellular CO_2 concentration (Ci) and chlorophyll (Chl) contentof hybrid poplar clone '546' (*Populusdeltoides cv. 55/56 x P. deltoides cv. Imperial*). Data shown are the mean ± standard deviation of three-OTC measurements. The letters on top of the bars are based on the Tukey test across the two measurements, with different letters indicating significantly different from each other at P<0.05.

Figure 3. Effects of ozone (CF, charcoal-filtered ambient air, and E-O_3, elevated O_3) and Nitrogen (N0, no N added, and N50, 50 kg N ha^{-1} yr^{-1}) on apoplastic NH_4^+ concentration, tissue NH_4^+ concentration, apoplastic pH and emission potential (Γ_s) of hybrid poplar clone '546' (*Populusdeltoides cv. 55/56 x P. deltoides cv. Imperial*). Data shown are the mean ± standard deviation of three-OTC measurements. The letters on top of the bars are based on the Tukey test across the two measurements, with different letters indicating significantly different from each other at P<0.05.

Figure 4. Effects of ozone (CF, charcoal-filtered ambient air, and E-O_3, elevated O_3) and Nitrogen (N0, no N added, and N50, 50 kg N ha^{-1} yr^{-1}) on the stomatal compensation point (χ_s)

Figure 5. Correlation between the stomatal compensation point (χ_s) and light-saturated photosynthesis (A_{sat}), stomatal conductance (g_s), intercellular CO_2 concentration (Ci) and chlorophyll (Chl) content across all ozone and nitrogen treatments. Green, red, blue and pink dots represent charcoal-filtered ambient air (CF)*N0 (no N added), CF*N50 (50 kg N ha^{-1} yr^{-1}), elevated O_3 (E-O_3)*N0 and E-O_3*N50 treatment, respectively. As

ANCOVA did not show significant differences in the slope of the regression lines for the individual O_3 or N treatments, one single line is shown.

Figure 6. Correlations between apoplastic pH and light-saturated photosynthesis (A_{sat}), chlorophyll (Chl) content, and intercellular CO_2 concentration (Ci), and correlation between apoplastic NH_4^+ concentration and leaf tissue NH_4^+ concentration across all ozone and nitrogen treatments. Green, red, blue and pink dots represent charcoal-filtered ambient air (CF)*N0 (no N added), CF*N50 (50 kg N ha^{-1} yr^{-1}), elevated O_3 (E-O_3)*N0 and E-O_3*N50 treatment, respectively. As ANCOVA did not show significant differences in the slope of the regression lines for the individual O_3 or N treatments, one single line is shown.

Figure 7. Actual forest distribution in China (a) (adopting from Li et al. (2017)) and atmospheric NH_3 concentration over deciduous broadleaf forests in July (b) and August (b) modeled using the GEOS-Chem model.

Figure 1

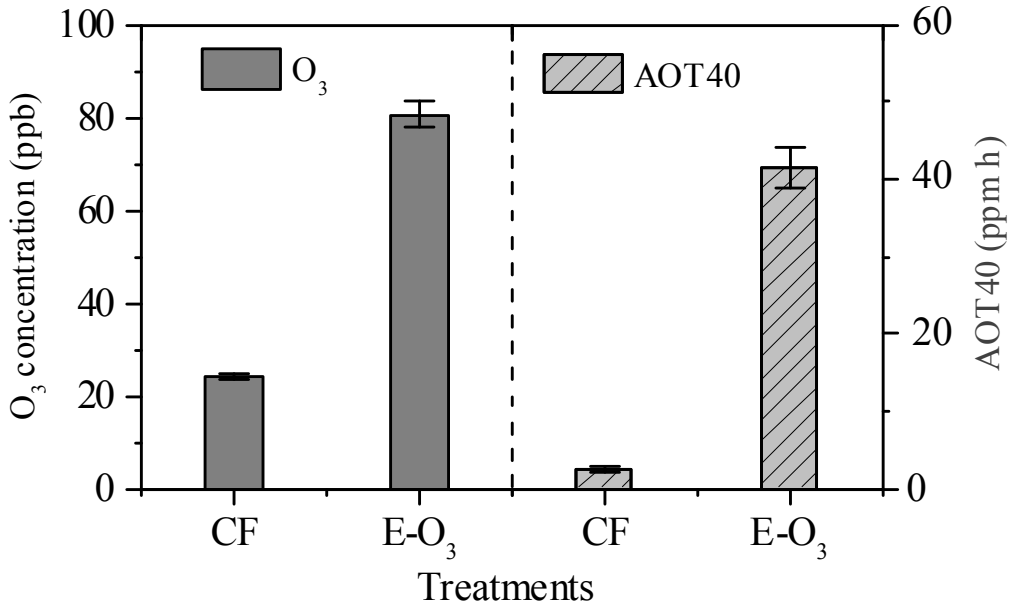
100
80
60
40
20
0
O_3 concentration (ppb)
60
40
20
0
AOT40 (ppm h)
O_3
AOT40
CF
E-O_3
CF
E-O_3
Treatments

Figure 2

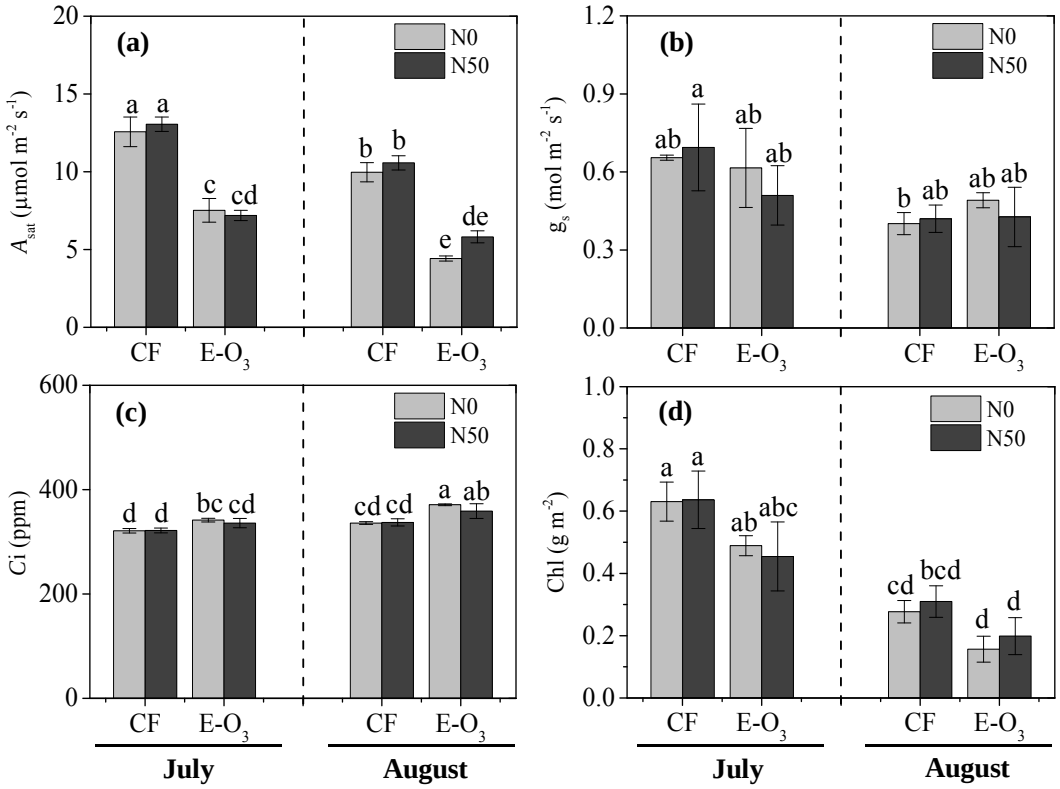
(a)
(b)
(c)
(d)
N0
N50
A_{sat} (μmol m^{-2} s^{-1})
g_s (mol m^{-2} s^{-1})
Ci (ppm)
Chl (g m^{-2})
CF
E-O$_3$
July
August

Figure 3

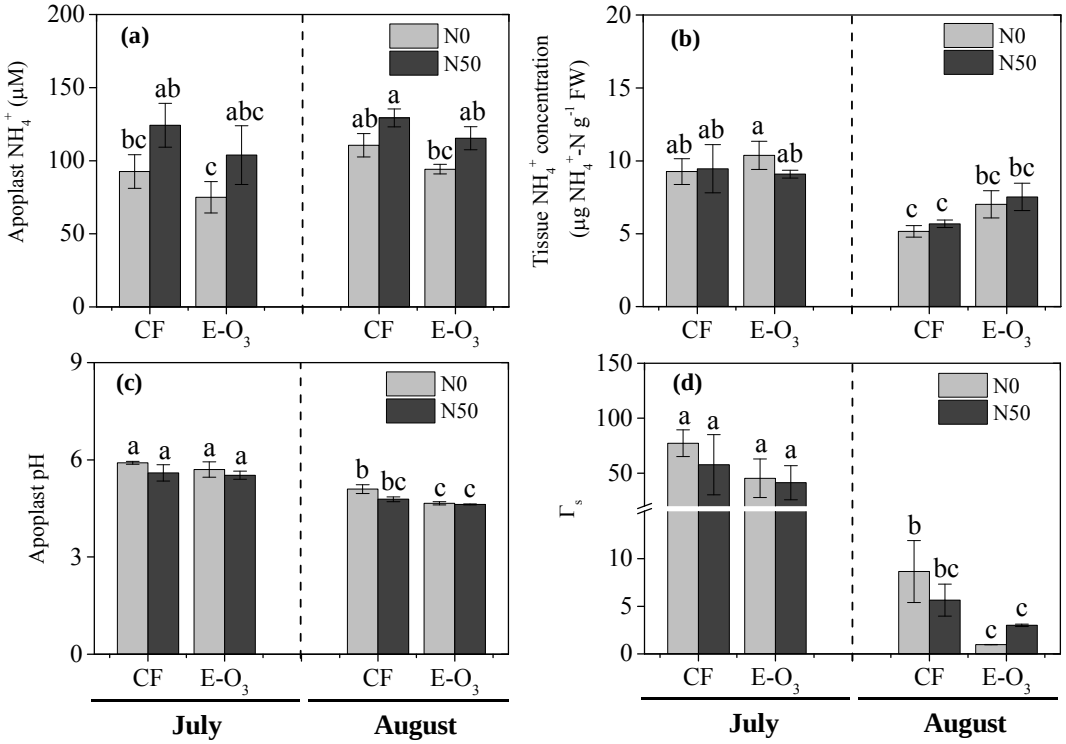
(a)
(b)
(c)
(d)
N0
N50
Apoplast NH4+ (μM)
Tissue NH4+ concentration (μg NH4+-N g-1 FW)
Apoplast pH
Γs
CF
E-O3
July
August

Figure 4

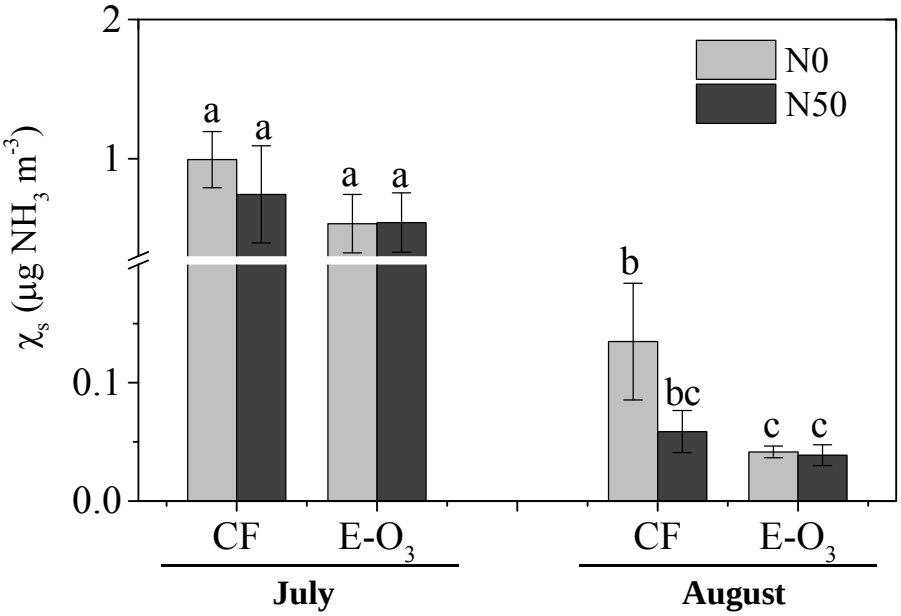
2
1
0.1
0.0
χ_s (µg NH_3 m^{-3})
N0
N50
a
a
a
a
b
bc
c
c
CF
E-O_3
CF
E-O_3
July
August

Figure 5

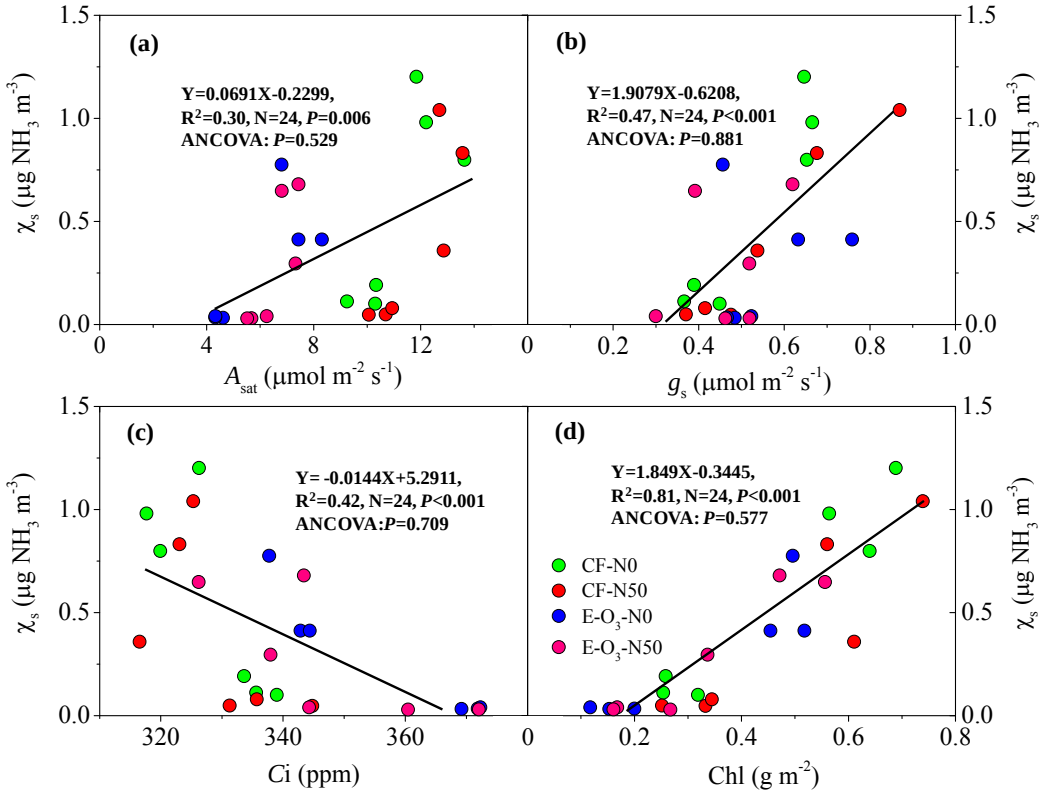
(a)
Y=0.0691X-0.2299,
R²=0.30, N=24, P=0.006
ANCOVA: P=0.529
(b)
Y=1.9079X-0.6208,
R²=0.47, N=24, P<0.001
ANCOVA: P=0.881
(c)
Y= -0.0144X+5.2911,
R²=0.42, N=24, P<0.001
ANCOVA:P=0.709
(d)
Y=1.849X-0.3445,
R²=0.81, N=24, P<0.001
ANCOVA: P=0.577
CF-N0
CF-N50
E-O3-N0
E-O3-N50
χs (μg NH3 m-3)
Asat (μmol m-2 s-1)
gs (μmol m-2 s-1)
Ci (ppm)
Chl (g m-2)

Figure 6

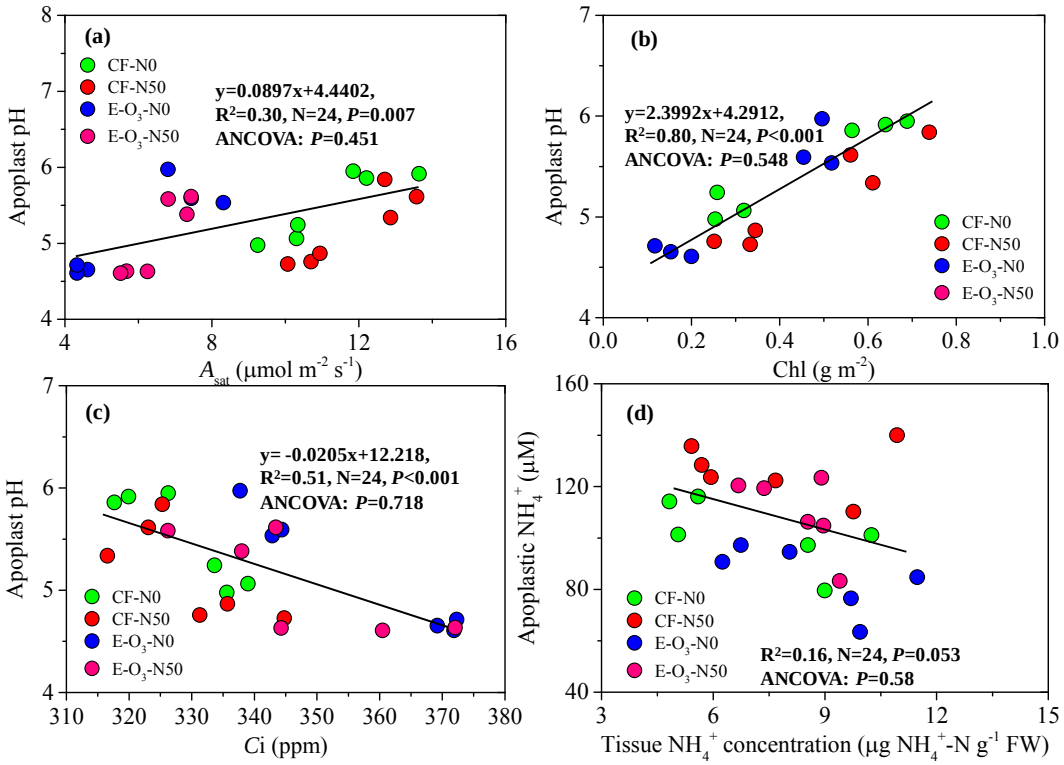
(a)
CF-N0
CF-N50
E-O3-N0
E-O3-N50
y=0.0897x+4.4402,
R2=0.30, N=24, P=0.007
ANCOVA: P=0.451
Apoplast pH
Asat (μmol m-2 s-1)
(b)
y=2.3992x+4.2912,
R2=0.80, N=24, P<0.001
ANCOVA: P=0.548
Chl (g m-2)
(c)
y= -0.0205x+12.218,
R2=0.51, N=24, P<0.001
ANCOVA: P=0.718
Ci (ppm)
(d)
R2=0.16, N=24, P=0.053
ANCOVA: P=0.58
Apoplastic NH4+ (μM)
Tissue NH4+ concentration (μg NH4+-N g-1 FW)

Figure 7

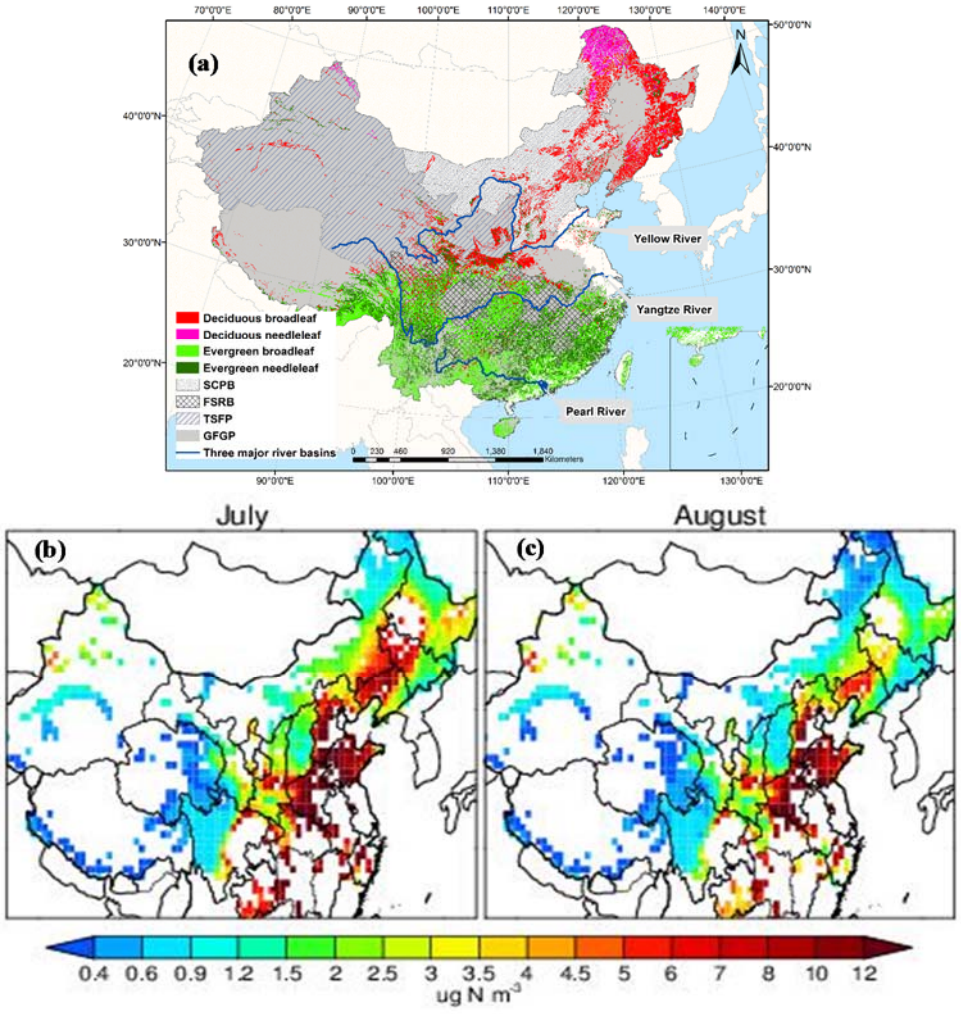
(a)
Deciduous broadleaf
Deciduous needleleaf
Evergreen broadleaf
Evergreen needleleaf
SCPB
FSRB
TSFP
GFGP
Three major river basins
Yellow River
Yangtze River
Pearl River
July
August
(b)
(c)
0.4 0.6 0.9 1.2 1.5 2 2.5 3 3.5 4 4.5 5 6 7 8 10 12
ug N m-3

Table 1. ANOVA results (*P* values) for the individual effects of interactions of O_3 (CF and E-O_3), N (N0 and N50), and sampling data (July and August) on light-saturated rate of CO_2 assimilation (*A*sat), stomatal conductance (g_s), intercellular CO_2 concentration (Ci), chlorophyll content (Chl), apoplastic pH, apoplastic NH_4^+, leaf tissue NH_4^+, potential emission (Γ_s), and stomatal compensation point (χ_s).

	O_3	N	Date (D)	O_3*N	O_3*D	N*D	O_3*N*D
*A*sat	**<0.001**	**0.034**	**<0.001**	0.980	0.518	0.064	0.104
g_s	0.432	0.503	**<0.001**	0.189	0.071	0.905	0.692
Ci	**<0.001**	0.150	**<0.001**	0.099	0.072	0.621	0.542
Chl	**<0.001**	0.674	**<0.001**	0.810	0.405	0.373	0.631
Apoplast pH	**0.001**	**0.003**	**<0.001**	0.080	0.103	0.777	0.482
Apoplast NH_4^+	**0.002**	**<0.001**	**0.011**	0.958	0.688	0.294	0.820
Leaf tissue NH_4^+	**<0.001**	0.119	**<0.001**	0.107	0.199	0.848	0.527
Γ_s	**0.009**	0.982	**<0.001**	0.347	0.062	0.175	0.326
χ_s	**<0.001**	0.059	**<0.001**	0.059	0.103	0.454	0.470

CF: charcoal-filtered ambient air; E-O_3: elevated O_3; N0: no N added; N50: 50 kg N ha^{-1} yr^{-1}; Statistically significant effects ($P<0.05$) are marked in bold.